

Title: Symmetry breaking in the female germline cyst

Authors: D. Nashchekin^{1*}, L. Busby¹, M. Jakobs², I. Squires^{1†} and D. St Johnston^{1*}

Affiliations:

¹The Gurdon Institute and the Department of Genetics, University of Cambridge; Tennis Court Road, Cambridge CB2 1QN, United Kingdom.

²The Department of Physiology, Development and Neuroscience, University of Cambridge; Cambridge CB2 3DY, United Kingdom.

*Corresponding author. Email: d.stjohnston@gurdon.cam.ac.uk,
d.nashchekin@gurdon.cam.ac.uk

†Present address: Institute for Cell and Molecular Biosciences, Newcastle University, Newcastle upon Tyne NE2 4HH, UK

Abstract: In mammals and flies, only one cell in a multicellular female germline cyst becomes an oocyte, but how symmetry is broken to select the oocyte is unknown. Here we show that the microtubule minus end-stabilizing protein, Patronin/CAMSAP marks the future *Drosophila* oocyte and is required for oocyte specification. The spectraplakins, Shot, recruits Patronin to the fusome, a branched structure extending into all cyst cells. Patronin stabilizes more microtubules in the cell with most fusome. Our data suggest that this weak asymmetry is amplified by Dynein-dependent transport of Patronin-stabilized microtubules. This forms a polarized microtubule network, along which Dynein transports oocyte determinants into the presumptive oocyte. Thus, Patronin amplifies a weak fusome anisotropy to break symmetry and select one cell to become the oocyte.

One-Sentence Summary: Patronin and Dynein form a positive feedback loop that amplifies a weak fusome asymmetry to specify the *Drosophila* oocyte.

Main Text: In many organisms, not all female germ cells develop into oocytes. Some cells become accessory cells that contribute material to the oocyte (1). Mouse female germ cells form cysts of up to 30 cells, but most cells undergo apoptosis after transferring cytoplasm and centrosomes to the small number of cells that become oocytes (2, 3). In *Drosophila*, germline cyst formation starts in the germarium, which has 3 regions. A stem cell produces a cystoblast, which then divides four times with incomplete cytokinesis to generate a cyst of 16 germ cells connected by intercellular bridges, “ring canals” (4, 5). As the cyst moves through regions 2a-b of the germarium, it is surrounded by epithelial follicle cells and then rounds up in region 3 to form a follicle. By this stage, one cell has been selected as the oocyte, whereas others become nurse cells (Fig. 1A). Oocyte selection depends on the formation of a noncentrosomal microtubule organizing center (ncMTOC) in the future oocyte that organizes a polarized microtubule network that directs the dynein-dependent transport of cell fate determinants and centrosomes into the pro-oocyte (6-8) (Fig. 1A). How symmetry is broken to specify which cell contains the ncMTOC and becomes the oocyte is unclear.

Patronin and its vertebrate orthologues (CAMSAPs) are microtubule minus end binding proteins that have been recently found to be essential components of ncMTOCs (9-13). To investigate the role of Patronin in oocyte determination, we examined the distribution of oocyte markers in *patronin*^{c9-c5} mutant cysts (Fig. 1B-C and S1). In wild-type cysts, Orb and centrosomes accumulate in future oocytes in regions 2b-3 (14-16), but they are rarely localized in *patronin* mutants (24% and 3% of mutant cysts respectively) (Fig. 1B-C). Several germ cells enter meiosis in region 2a and accumulate the synaptonemal complex protein C(3)G. C(3)G becomes restricted to two cells in region 2b and to the oocyte in region 3 (17) (Fig. S1). C(3)G is not localized in region 3 of *patronin* cysts and 44% of the cysts in region 2b have 3 cells in meiosis (Fig. S1). Thus, Patronin is required for oocyte determination.

To examine whether Patronin is asymmetrically distributed in the cyst, we imaged germaria expressing endogenously tagged Patronin-Kate. Patronin starts to accumulate in a single cell in each cyst in region 2a, earlier than other markers for the presumptive oocyte, and remains in one cell in regions 2b-3, where it forms distinct foci in the cytoplasm (Fig. 2A-2A'). This cell will become the oocyte, as it is also labelled by Orb (Fig. 2B) and C(3)G (Fig. 2C). *patronin* mRNA is not localized within the cyst and Patronin expressed from a cDNA with heterologous UTRs and promoter shows a similar distribution to the endogenous protein, indicating that Patronin is localized as a protein and not through transcription in this cell or mRNA localization (Fig. 2B-C and Fig. S2).

Dynein does not localize to the presumptive oocyte in *patronin* mutant cysts (Fig. 3A). This suggests that the loss of Patronin disrupts the formation of the MTOC in the pro-oocyte, leading to loss of the polarized microtubule network along which Dynein transports cargoes into one cell. As most of MT plus ends accumulate at the site of MT nucleation, we used the MT plus end-tracking protein EB1-GFP to visualize the putative MTOC in the cyst. The majority of EB1-GFP comets localize to one cell in regions 2b-3 (Fig. 3B-C, Movies S1-S2). Moreover, the densest EB1-GFP signal co-localizes with the Patronin foci in the same cell, suggesting that the latter are the MTOCs formed in the pro-oocyte (Fig. 3D). This asymmetric distribution of EB1-GFP is lost in *patronin* cysts, where EB1-GFP comets are distributed more homogeneously (Fig. 3B-C, Movies S3-S4). Patronin is therefore required for MTOC formation in the presumptive oocyte and the organization of a polarized MT network.

Wild-type cysts contain a population of stable, acetylated MTs that form along the fusome, an ER, spectrin, and actin-rich structure that connects all cells of the cyst (16-19) (Fig. S3). In

patronin mutant cysts, there is a 2.5 fold reduction in stable MTs (Fig. 3E and S3). Thus, in the absence of Patronin, the whole organization of MTs in the cyst is disrupted. Patronin binds MT minus ends and stabilizes MTs by protecting their minus ends against kinesin-13 induced depolymerization (11, 13). Our results suggest that early accumulation of Patronin in only one cell of the cyst stabilizes MT minus ends there, leading to dynein-dependent transport into this cell, the formation of MTOCs and the subsequent specification of the oocyte.

To examine whether centrosomes contribute to the formation of Patronin MTOCs, we imaged cysts expressing endogenously tagged Patronin-YFP and the centrosomal protein Asterless-Cherry. Although centrosomal clusters localize near Patronin foci, the Asterless and Patronin signals only partially overlap and most Patronin foci lie outside the centrosomal cluster, indicating that Patronin MTOCs are noncentrosomal (Fig. S4A). Centrosomes have been proposed to be inactive during their migration into the oocyte, and they lack crucial components of the PCM (8). To test whether centrosomes contribute to microtubule organization, we imaged cysts expressing EB1-GFP and Asterless-Cherry. The centrosomes show strong MT nucleating activity in region 1, where they organize the mitotic spindles (Fig. S4B and Movie S5). However, only some Asterless-Cherry labelled centrosomes in the presumptive oocyte produce EB1-GFP comets in region 2b (Fig. S4C and Movie S6). Thus, Patronin-dependent ncMTOCs create the initial asymmetry in MT organization that leads to the accumulation of centrosomes in the pro-oocyte, which may then be amplified by activation of some centrosomes in this cell. The close proximity of the active centrosomes to the ncMTOCs, raises the possibility that new MTs produced by these centrosomes are released and then captured and stabilized by Patronin in ncMTOCs, a mechanism described for CAMSAP proteins (20).

The observation that Patronin is the earliest known marker for the future oocyte raises the question of how symmetry is broken in the cyst to enrich Patronin in one cell. One proposed mechanism for symmetry-breaking is that the cell that inherits the most fusome becomes the presumptive oocyte (21). The fusome is asymmetrically partitioned during the mitoses in region 1, so that mother cells inherit more material than their daughters and one of the two cells with four ring canals has more fusome than the rest (19). To examine whether Patronin associates with the fusome, we imaged germaria expressing endogenously-tagged Patronin-YFP and the fusome marker, Hts-Cherry. Patronin localizes on the fusome in early region 2a, but becomes concentrated in one cell as the cyst progresses towards region 3 (Fig. 4A and S5A). When the MTs are depolymerized with colcemid, however, Patronin remains on the fusome in regions 2b-3 (Fig. 4B). Thus, the fusome determines the initial localization of Patronin in early region 2a, including its slight enrichment in the pro-oocyte, which is then amplified by a MT-dependent process.

The spectraplaklin Shot, localizes to the fusome, is required for the oocyte specification, and recruits Patronin to ncMTOCs in the oocyte later in oogenesis, making it a good candidate for a factor that links Patronin to the fusome (13, 17). In *shot* cysts, Patronin does not accumulate in one cell and fails to form foci (Fig. 4C). Furthermore, loss of Shot prevents Patronin from associating with the fusome (Fig. 4C, S5B-C). Thus, Shot is required to recruit Patronin to the fusome, thereby transmitting fusome asymmetry to Patronin localization.

The MT-dependent enrichment of Patronin in one cell as the cyst moves through the germarium suggests its initial, weakly asymmetric distribution on the fusome is then amplified by Dynein-dependent transport towards the minus ends of the MT that have been stabilized by Patronin. We

tested Dynein function by examining components of the Dynein/dynactin complex that are required for oocyte specification: *egl*, *BicD* and *Arp1* (22-24), (Fig. 4D, S6A-6B). Like MT depolymerization, mutations in any of these genes disrupt the enrichment of Patronin foci in one cell. Deletion of the MT minus end-binding domain of Patronin, but not the CKK domain (25), also prevents Patronin accumulation in the pro-oocyte (Fig. S6C-D). Thus, Patronin localization depends on its binding to MT minus ends and on Dynein activity, suggesting that Dynein transports Patronin bound to MT minus ends towards the pro-oocyte.

Our observations lead us to propose a 4-step model of cyst polarization and oocyte selection (Fig. 4E). First, during cyst formation, the asymmetric segregation of the fusome leads to the one cell with more fusome material than the rest. Second, in region 2a, Patronin is recruited to the fusome by Shot. The cell with most fusome therefore contains more Patronin, leading to the stabilization of more MT minus ends in this cell and a weakly polarized MT network. Third, Patronin bound MTs in other cells of the cyst are then transported by Dynein along these MTs towards their minus ends in the pro-oocyte. Fourth, this creates a positive feedback loop: as Dynein transports more Patronin and MTs into the cell with most stabilized MT minus ends, more minus ends become stabilized in this cell, amplifying the MT polarity and leading to enhanced Dynein transport of oocyte determinants into this cell. In this way, the small original asymmetry in the fusome is converted into the highly polarized MT network that concentrates the oocyte determinants in one cell.

Patronin is a member of the conserved CAMSAP family, raising the possibility that the molecular mechanisms of oocyte selection in *Drosophila* could be conserved during the formation of mammalian oocytes. Although fusomes have not been observed in mammalian

cysts (26), MT-dependent transport of organelles through intercellular bridges has been shown to play an important role in oocyte differentiation in mice (3).

References and Notes

1. K. Lu, L. Jensen, L. Lei, Y. M. Yamashita, Stay Connected: A Germ Cell Strategy. *Trends Genet.* **33**, 971–978 (2017).
2. L. Lei, A. C. Spradling, Mouse primordial germ cells produce cysts that partially fragment prior to meiosis. *Development.* **140**, 2075–2081 (2013).
3. L. Lei, A. C. Spradling, Mouse oocytes differentiate through organelle enrichment from sister cyst germ cells. *Science.* **352**, 95–99 (2016).
4. M. de Cuevas, M. A. Lilly, A. C. Spradling, Germline cyst formation in *Drosophila*. *Annu. Rev. Genet.* **31**, 405–28 (1997).
5. J. Huynh, D. StJohnston, The Origin of Asymmetry: Early Polarisation of the *Drosophila* Germline Cyst and Oocyte. *Current Biology.* **14**, R438–R449 (2004).
6. W. E. Theurkauf, B. M. Alberts, Y.-N. Jan, T. A. Jongens, A central role for microtubules in the differentiation of *Drosophila* oocytes. *Development.* **118**, 1169–1180 (1993).
7. M. McGrail, T. S. Hays, The microtubule motor cytoplasmic dynein is required for spindle orientation during germline cell divisions and oocyte differentiation in *Drosophila*. *Development.* **124**, 2409–2419 (1997).
8. J. Bolivar *et al.*, Centrosome migration into the *Drosophila* oocyte is independent of BicD and egl, and of the organisation of the microtubule cytoskeleton. *Development.* **128**, 1889–1897 (2001).
9. W. Meng, Y. Mushika, T. Ichii, M. Takeichi, Anchorage of microtubule minus ends to adherens junctions regulates epithelial cell-cell contacts. *Cell.* **135**, 948–959 (2008).
10. A. J. Baines *et al.*, The CKK Domain (DUF1781) Binds Microtubules and Defines the CAMSAP/spp4 Family of Animal Proteins. *Molecular Biology and Evolution.* **26**, 2005–2014 (2009).
11. S. S. Goodwin, R. D. Vale, Patronin Regulates the Microtubule Network by Protecting Microtubule Minus Ends. *Cell.* **143**, 263–274 (2010).
12. N. Tanaka, W. Meng, S. Nagae, M. Takeichi, Nezha/CAMSAP3 and CAMSAP2 cooperate in epithelial-specific organization of noncentrosomal microtubules. *Proc Natl Acad Sci USA.* **109**, 20029–20034 (2012).
13. D. Nashchekin, A. R. Fernandes, D. St Johnston, Patronin/Shot Cortical Foci Assemble the Noncentrosomal Microtubule Array that Specifies the *Drosophila* Anterior-Posterior Axis. *Dev Cell.* **38**, 61–72 (2016).
14. V. Lantz, J. S. Chang, J. I. Horabin, D. Bopp, P. Schedl, The *Drosophila* orb RNA-binding protein is required for the formation of the egg chamber and establishment of polarity. *Genes Dev.* **8**, 598–613 (1994).

15. A. P. Mahowald, J. M. Strassheim, Intercellular migration of centrioles in the germarium of *Drosophila melanogaster*. An electron microscopic study. *The Journal of Cell Biology*. **45**, 306–320 (1970).
- 5 16. N. C. Grieder, M. de Cuevas, A. C. Spradling, The fusome organizes the microtubule network during oocyte differentiation in *Drosophila*. *Development*. **127**, 4253–4264 (2000).
17. K. Roper, N. H. Brown, A spectraplakin is enriched on the fusome and organizes microtubules during oocyte specification in *Drosophila*. *Curr Biol*. **14**, 99–110 (2004).
- 10 18. H. Lin, L. Yue, A. C. Spradling, The *Drosophila* fusome, a germline-specific organelle, contains membrane skeletal proteins and functions in cyst formation. *Development*. **120**, 947–956 (1994).
19. M. De Cuevas, A. C. Spradling, Morphogenesis of the *Drosophila* fusome and its implications for oocyte specification. *Development*. **125**, 2781–2789 (1998).
- 15 20. K. Jiang *et al.*, Microtubule minus-end stabilization by polymerization-driven CAMSAP deposition. *Dev Cell*. **28**, 295–309 (2014).
21. H. Lin, A. C. Spradling, Fusome asymmetry and oocyte determination in *Drosophila*. *Developmental Genetics*. **16**, 6–12 (1995).
22. C. Navarro, H. Puthalakath, J. M. Adams, A. Strasser, R. Lehmann, Egalitarian binds dynein light chain to establish oocyte polarity and maintain oocyte fate. *Nat Cell Biol*. **6**, 427–435 (2004).
- 20 23. B. Suter, R. Steward, Requirement for phosphorylation and localization of the Bicaudal-D protein in *Drosophila* oocyte differentiation. *Cell*. **67**, 917–926 (1991).
24. R. Nieuwburg *et al.*, Localised dynactin protects growing microtubules to deliver oskar mRNA to the posterior cortex of the *Drosophila* oocyte. *Elife*. **6**, e27237 (2017).
- 25 25. M. C. Hendershott, R. D. Vale, Regulation of microtubule minus-end dynamics by CAMSAPs and Patronin. *Proceedings of the National Academy of Sciences*. **111**, 5860–5865 (2014).
26. M. E. Pepling, A. C. Spradling, Female mouse germ cells form synchronously dividing cysts. *Development*. **125**, 3323–3328 (1998).
- 30 27. K. Roper, N. H. Brown, Maintaining epithelial integrity: a function for gigantic spectraplakin isoforms in adherens junctions. *Journal of Cell Biology*. **162**, 1305–1315 (2003).
28. B. Ran, R. Bopp, B. Suter, Null alleles reveal novel requirements for Bic-D during *Drosophila* oogenesis and zygotic development. *Development*. **120**, 1233–1242 (1994).
- 35 29. S. T. Thibault *et al.*, A complementary transposon tool kit for *Drosophila melanogaster*

using P and piggyBac. *Nature Genetics*. **36**, 283–287 (2004).

30. T. Schupbach, E. Wieschaus, Female sterile mutations on the second chromosome of *Drosophila melanogaster*. II. Mutations blocking oogenesis or altering egg morphology. *Genetics*. **129**, 1119–1136 (1991).

5 31. F. Port, H.-M. Chen, T. Lee, S. L. Bullock, Optimized CRISPR/Cas tools for efficient germline and somatic genome engineering in *Drosophila*. *Proceedings of the National Academy of Sciences*. **111**, E2967–76 (2014).

10 32. N. Lowe *et al.*, Analysis of the expression patterns, subcellular localisations and interaction partners of *Drosophila* proteins using a pigP protein trap library. *Development*. **141**, 3994–4005 (2014).

33. G. B. Gloor, N. A. Nassif, D. M. Johnson-Schlitz, C. R. Preston, W. R. Engels, Targeted gene replacement in *Drosophila* via P element-induced gap repair. *Science*. **253**, 1110–1117 (1991).

15 34. P. T. Conduit, A. Wainman, Z. A. Novak, T. T. Weil, J. W. Raff, Re-examining the role of *Drosophila* Sas-4 in centrosome assembly using two-colour-3D-SIM FRAP. *Elife*. **4** (2015), doi:10.7554/eLife.08483.

35. T. Zhao, O. S. Graham, A. Raposo, D. St Johnston, Growing microtubules push the oocyte nucleus to polarize the *Drosophila* dorsal-ventral axis. *Science*. **336**, 999–1003 (2012).

20 36. H. Wang, I. Brust-Mascher, G. Civelekoglu-Scholey, J. M. Scholey, Patronin mediates a switch from kinesin-13-dependent poleward flux to anaphase B spindle elongation. *The Journal of Cell Biology*. **4**, 1343 (2013).

37. T. B. Chou, N. Perrimon, Use of a yeast site-specific recombinase to produce female germline chimeras in *Drosophila*. *Genetics*. **131**, 643–653 (1992).

25 **Acknowledgments:** We are grateful to R. Hawley, J. Raff, J. Scholey and the Bloomington Stock Center (NIH P40OD018537) for flies and reagents, the Gurdon Institute Imaging Facility for assistance with microscopy, N. Lowe and J. Overton for technical assistance. **Funding:** Wellcome Principal Research Fellowship 080007 and 207496 (DSJ), Wellcome core support 092096 and 203144 (DSJ), Wellcome PhD studentship 109145 (MJ), Cancer Research UK core support A14492 and A24823 (DSJ), BBSRC grant BB/R001618/1 (DSJ, DN, IS). **Author contributions:** Conceptualization: DN, DSJ; Methodology: DN, MJ. Investigation: DN, LB, MJ, IS, DSJ. Visualization: DN, MJ, DSJ. Funding acquisition: DN, DSJ. Project administration: DN, DSJ. Supervision: DN, DSJ. Writing – original draft: DN, DSJ. Writing – review & editing: DN, LB, MJ, IS, DSJ. **Competing interests:** Authors declare that they have no competing interests. **Data and materials availability:** All data are available in the main text or the supplementary materials.

30
35

Supplementary Materials

Materials and Methods

Supplementary text

Figs. S1 to S6

5 References (27–37)

Movies S1 to S6

Fig. 1. Patronin is required for the oocyte specification. (A) A schematic diagram of a *Drosophila* germarium showing germline cyst formation and oocyte selection. Distribution of the oocyte specification markers Orb (B) and centrosomes (C) in wild type (WT; top or left in C) and *patronin* mutant (bottom or right in C) cysts. For all figures: arrows point to the future oocyte; cysts are marked by dashed lines; mutant cysts are labeled by the absence of nlsRFP; regions of the germarium are indicated on the top; scale bars, 10µm.

15

Fig. 2. Patronin accumulates in the future oocyte. (A-A') Two different focal planes of a live germarium showing accumulation of endogenously tagged Patronin-Kate in one cell of the cyst. Regions 2a and 2b are shown as close-ups. Cell membranes are labelled by Basigin-YFP (Bsg-YFP). (B-C) Ectopically-expressed *ubq>Patronin-GFP* accumulates in future oocytes labelled by Orb (B) or C(3)G (C).

20

Fig. 3. Patronin is required for MT organisation in the cyst. (A) Distribution of Dynein Heavy Chain (DHC) in wild type (WT) and *patronin* mutant cysts. (B-D) Patronin is required for MTOC formation in the presumptive oocyte. (B) EB-1 comet tracks in wild type (WT; top) and *patronin* mutant (bottom) cysts. The images are projections of several time points from Movies

25

S1 (WT; region 2), S2 (WT; region 3), S3 (*patronin*; region 2) and S4 (*patronin*; region 3). The red dashed line marks cells with MTOCs. **(C)** Quantification of EB-1 comet distribution in wild type (WT) and *patronin* mutant cysts in region 3 and 2b of germarium. Red dots indicate median values. **(D)** Live germarium showing co-localization of Patronin-YFP foci with the microtubules plus end marker EB1-GFP in the presumptive oocyte. **(E)** Quantification of the mean fluorescence intensities of fusome associated acetylated microtubules in *patronin* mutant and WT cysts. Error bars indicate the SEM.

Fig. 4. Patronin localisation is defined by fusome and by a positive feed back loop of Dynein mediated transport. **(A-B)** Patronin associates with the fusome in a microtubule-dependent manner. Untreated **(A)** or colcemid-treated **(B)** live germlaria expressing Patronin-YFP and Hts-Cherry. Regions 2a and 2b are shown as close-ups. **(C)** Shot links Patronin to the fusome. Live germlaria containing wild type (WT; left) and *shot* mutant (right) cysts expressing Patronin-YFP either untreated (top) or treated with colcemid (bottom). **(D)** Patronin localisation depends on Dynein activity. Wild type (WT; top) and *egalitarian* mutant (bottom) live germlaria expressing transgenic Patronin-GFP. **(E)** A diagram showing the 4 steps in cyst polarization that lead to the specification of the oocyte and its subsequent positioning at the posterior of the cyst in region 3. See text for details. Asterisk indicates the presumptive oocyte.

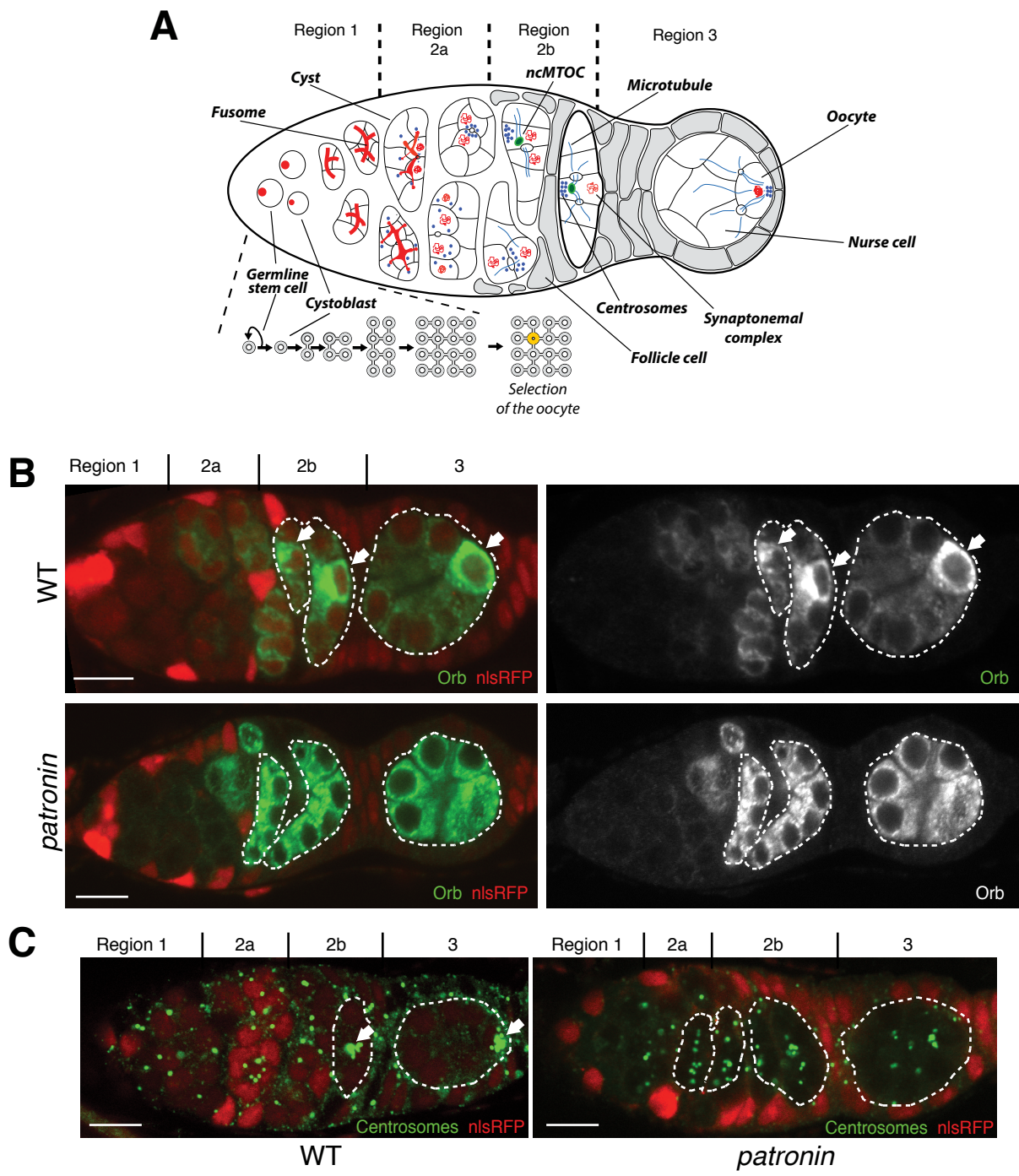


Figure 1

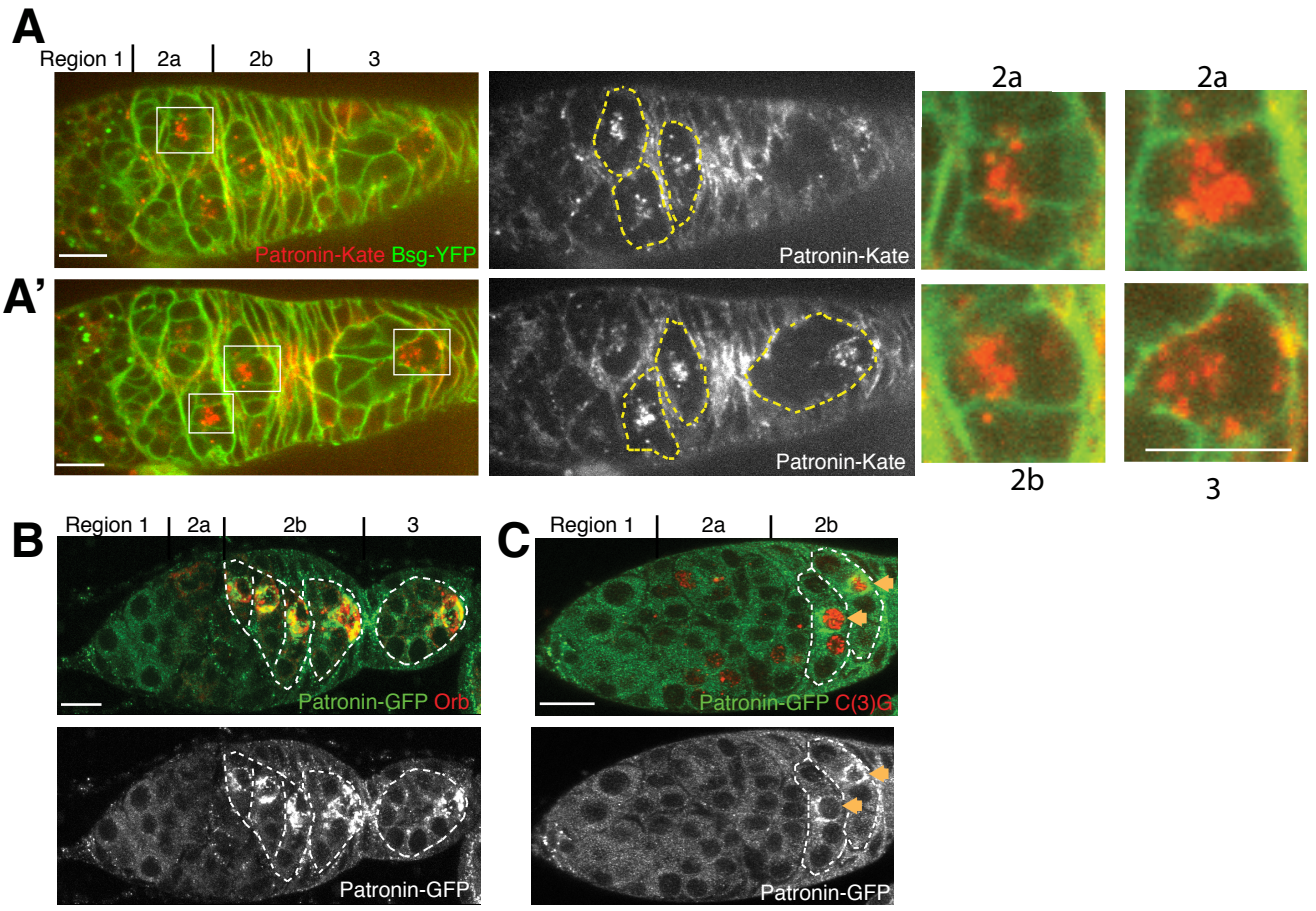


Figure 2

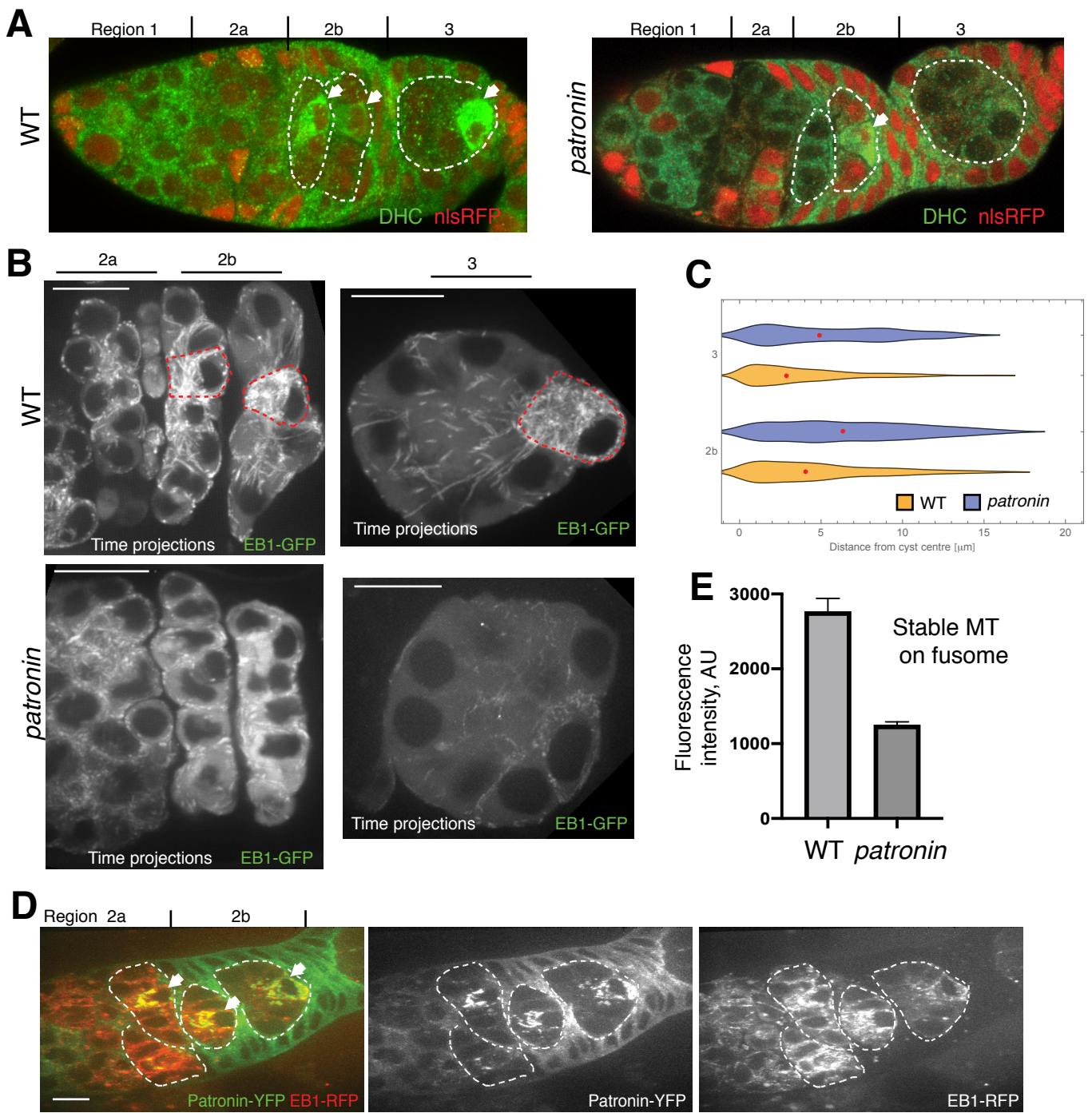


Figure 3

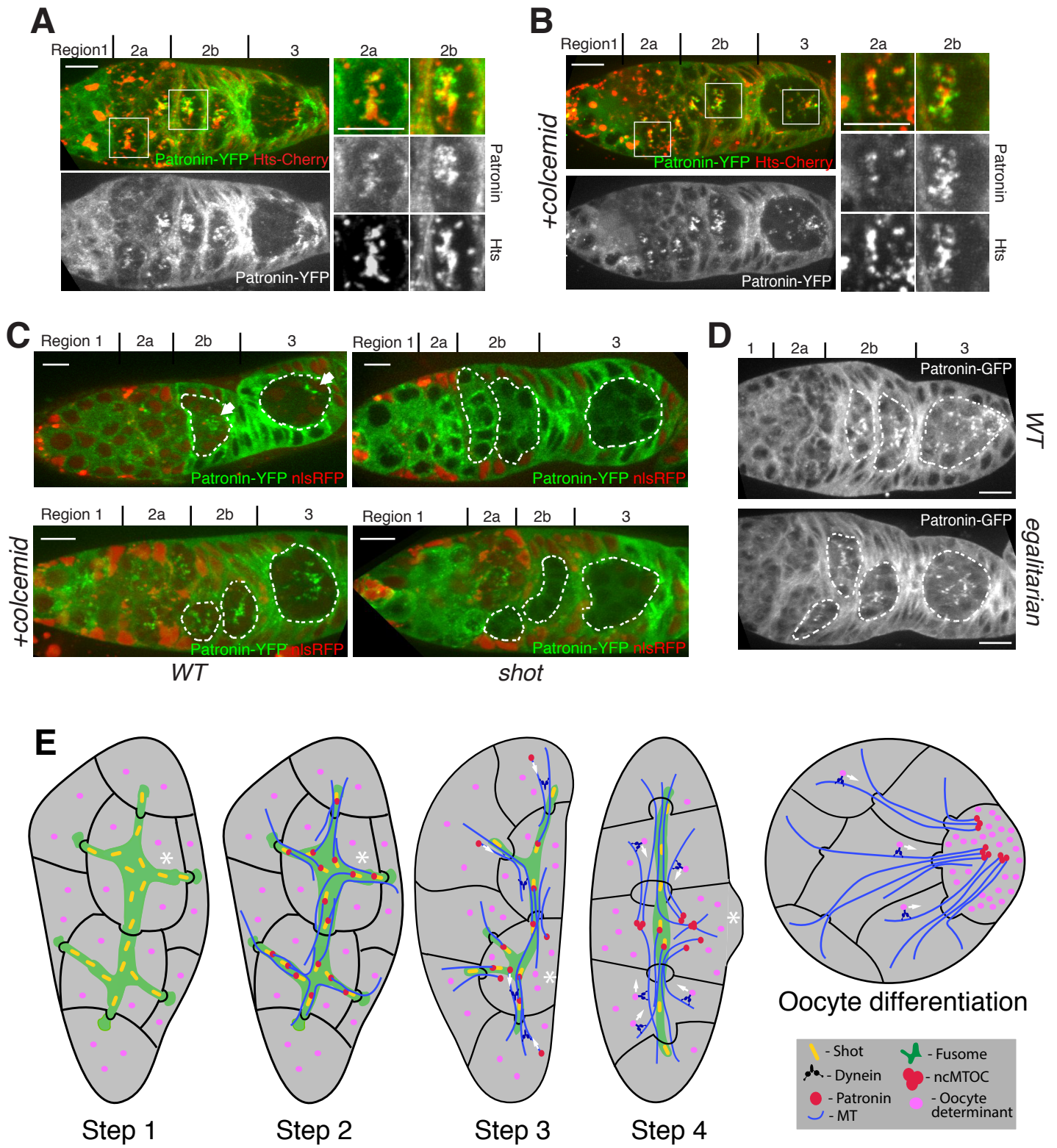


Figure 4



Supplementary Materials for

Symmetry breaking in the female germline cyst

D. Nashchekin, L. Busby, M. Jakobs, I. Squires and D. St Johnston

Correspondence to: : d.stjohnston@gurdon.cam.ac.uk, d.nashchekin@gurdon.cam.ac.uk

This PDF file includes:

Materials and Methods
Supplementary text
Figs. S1 to S6
Captions for Movies S1 to S6
References

Other Supplementary Materials for this manuscript include the following:

Movies S1 to S6

Materials and Methods

Mutant alleles. The following *Drosophila melanogaster* mutant alleles have been described previously and can be found on FlyBase.org: *shot*³ (27), *BicD*^{r5} (28), *arp1*^{c04425} (29), *egalitarian*¹ and *egalitarian*² (30). The *patronin*^{c9-c5} allele was generated by injecting nos::Cas9 embryos (31) with a sgRNA targeting the second protein coding exon in *patronin* (5' GGACATGCCCATACCGAAA 3'). *patronin*^{c9-c5} has a GC (highlighted in bold in the sgRNA sequence) to TA substitution changing Met Pro to Ile Ser; and a deletion of a G (highlighted in bold in sgRNA sequence) changing Glu Thr Val Leu to Lys Arg Tyr STOP, creating a premature stop codon after 105 amino acids. *patronin*^{c9-c5} is homozygous lethal. The mutant phenotypes of *patronin*^{c9-c5} were rescued by ubq>Patronin-GFP transgene.

Fluorescent marker stocks. Hts-Cherry was derived by N. Lowe from the Hts-GFP CPTI protein trap line using P-element exchange (32, 33). Basigin-YFP is Cambridge Protein Trap Insertion line (32). The following stocks have been described previously: Asterless-Cherry (34), UAS EB1-GFP (35), Patronin-YFP (13), pUbq-Patronin-GFP (36) (A isoform), Patronin-mKate, UAS EB1-RFP, pUbq-Patronin-GFP (I isoform), pUbq-PatroninΔMTD-GFP, pUbq-PatroninΔCKK-GFP were from this study.

Drosophila genetics. Germline clones of *patronin*^{c9-c5}, *shot*³, *BicD*⁵, *arp1*^{c04425} were induced by incubating larvae at 37° for two hours per day over a period of three days. Clones were generated with FRT G13 nlsRFP, FRT 40A nlsRFP, FRT 82B nlsRFP (Bloomington Stock Center) using the heat shock Flp/FRT system (37). Germline expression of UAS EB1-GFP and UAS EB1-RFP was induced by nanos-Gal4.

Molecular Biology. The Patronin C-terminal mKate knockin was made by injecting nos::Cas9 embryos (31) with a single guide RNA targeting the region of the stop codon in *patronin* (5' -GGCGCTTGTAATCTAAGCGG-3') and a donor plasmid with 4-kb homology arms surrounding the mKate sequence. Patronin-mKate is homozygous viable. A full-length *patronin* RI cDNA was amplified from pUASP mCherry-Patronin (13) and cloned together with EGFP into pUbq-attb vector downstream of the polyubiquitin promoter. pUbq-PatroninΔMTD-GFP and pUbq-PatroninΔCKK-GFP were generated by PCR amplifying the

corresponding fragments (see Ref (25) for details) from pUbq-Patronin-GFP and cloning them into pUbq-attb. EB1 cDNA was amplified from pUASP EB1-GFP and cloned together with tagRFP into pUASP-attb to generate UAS EB1-RFP.

Immunohistochemistry. Ovaries were fixed for 20 min in 4% paraformaldehyde and 0.2% Tween in PBS. Ovaries were then blocked with 1% BSA in PBS for 1 hr at room temperature. Ovaries were incubated with the primary antibody for 16 hr with 0.1% BSA in PBS with 0.2% Tween at 4C and for 4 hr with the secondary antibody at room temperature. We used the following primary antibodies: mouse anti-acetylated tubulin at 1:250 (Sigma); mouse anti-Dynein heavy chain at 1:50 (DSHB Hybridoma Product 2C11-2. Deposited to the DSHB by Scholey, JM); guinea pig anti-Shot (*13*) at 1:500, rabbit anti-dPLP at 1:1000 (gift from J. Raff, University of Oxford, UK), mouse anti-C(3)G at 1:500 (gift from R.S. Hawley, Stowers Institute, US), mouse anti-Orb at 1:10 (DSHB Hybridoma Products 4H8 and 6H4. Deposited to the DSHB by Schedl, P), mouse anti- α Spectrin at 1:200 (DSHB Hybridoma Product 3A9. Deposited to the DSHB by Branton, D. / Dubreuil, R.) Conjugated secondary antibodies (Jackson ImmunoResearch) were used at 1:100. In situ hybridizations were performed as previously described (24) .

Colcemid Treatment. Flies were starved for 2 hr and then fed colcemid (Sigma) in yeast paste (66 μ g/ml) for 17 hr. Ovaries were dissected and imaged as described below.

Imaging. For live imaging, ovaries were dissected and imaged in Voltalef oil 10S (VWR International) on an Olympus IX81 inverted microscope with a Yokogawa CSU22 spinning disk confocal imaging system (60x/ 1.35 NA Oil UPlanSApo and 100x/ 1.3 NA Oil UPlanSApo) or on Leica SP5 confocal microscope (63x/1.4 HCX PL Apo CS Oil). To label cell membranes, ovaries were dissected in Schneider's medium (Sigma) with 10 μ g/ml insulin (Sigma) and CellMask (1:2000, Life Technologies), incubated for 10 min at room temperature, washed and transferred to Voltalef oil for imaging. Fixed preparations were imaged using an Olympus IX81 (60x/ 1.35 NA Oil UPlanSApo) or a Leica SP8 (63x/1.4 HCX PL Apo CS Oil) confocal microscope. Images were collected with Olympus Fluoview, MetaMorph and Leica LAS AF software and processed using ImageJ. Germaria were imaged by collecting 10–15 z sections spaced 0.5 μ m apart. The images in Fig. 2B, Fig. 3A,

Fig. 4A, Fig. 4B, Fig. 4C (bottom panels) and Fig. 4D are projections of several z sections.

EB1 tracking. EB1 comets were tracked using the ImageJ plugin TrackMate. For each movie, tracking performance was visually inspected and optimal tracking parameters chosen accordingly. To determine the distribution of EB1 comets in the cyst we calculated the distance from each EB1 track starting point to the cyst centre. The following number of comets were analysed: WT region 3: 910 comets, WT region 2b: 430 comets; *patronin* mutant region 3: 989 comets, *patronin* mutant region 2b: 1736 comets.

Statistical analyses. The chi-square test was used to test whether values were significantly different between WT and *patronin* mutant cysts. The Mann-Whitney t-test was used to determine significance when comparing fluorescence intensities of acetylated tubulin staining and when measuring the co-localisation of fusome and Patronin. We used the MATLAB implementation of the Kruskal Wallis Test followed by a Tukey post hoc test to determine statistical differences in EB-1 comet distributions. A level of $p < 0.01$ was considered to be statistically significant. No statistical methods were used to predetermine sample size, the experiments were not randomized, and the investigators were not blinded to allocation during experiments and outcome assessment.

Reproducibility of experiments. Images are representative examples from at least three independent repeats for each experiment. The number of cysts analyzed for each experiment were as follows: Fig. 1B (WT 27, *patronin* 27), Fig. 1C (WT 30, *patronin* 41), Fig. S1 (WT 33, *patronin* 31), Fig. 2A (17), Fig. 2B (53), Fig. 2C (32), Fig. 3A (WT 19, *patronin* 14), Fig. 3B (WT 30, *patronin* 29), Fig. 3D (41), Fig. S3 (WT 40, *patronin* 45), Fig. 3E (WT 18, *patronin* 6), Fig. 4A (30), Fig. 4B (54), Fig. 4C (WT 35, WT + colcemid 37, *shot* 28, *shot* + colcemid 31), Fig. S5B (15), Fig. S5C (26), Fig. 4D (WT 40, *egalitarian* 34).

Supplementary text

Author contributions:

Conceptualization: DN, DStJ

Methodology: DN, MJ

Investigation: DN, LB, MJ, IS, DStJ

Visualization: DN, MJ, DStJ

Funding acquisition: DN, DStJ

Project administration: DN, DStJ

Supervision: DN, DStJ

Writing – original draft: DN, DStJ

Writing – review & editing: DN, LB, MJ, IS, DStJ

Competing interests: Authors declare that they have no competing interests.

Data and materials availability: All data are available in the main text or the supplementary materials.

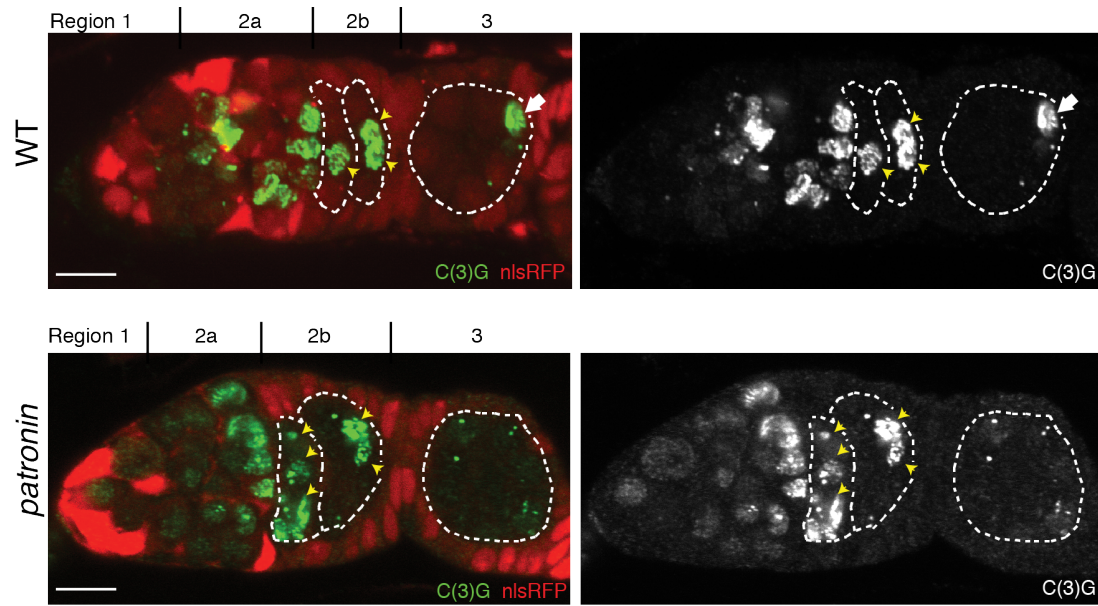


Fig. S1. Patronin is required for the oocyte specification. Distribution of oocyte specification marker C(3)G in wild type (WT; top) and *patronin* mutant (bottom) cysts. Arrows point to the future oocyte. Cysts are marked by dashed lines. Mutant cysts are labeled by the absence of nlsRFP. Arrowheads indicate cells accumulating C(3)G. Regions of the germarium are indicated on the top. Scale bars, 10 μ m.

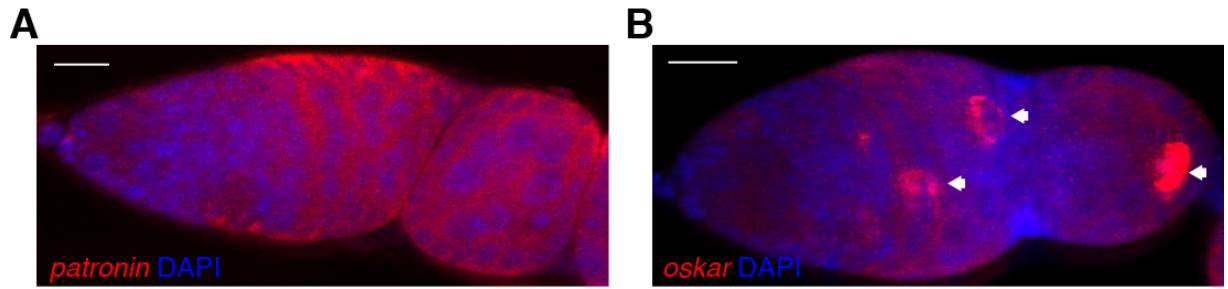


Fig. S2. Patronin mRNA is not localised in the cyst. Confocal images of fluorescent in situ hybridisations (FISH) to endogenous *patronin* (A) and *oskar* (B) mRNA in a wild type germarium, counterstained with DAPI to label the nuclei. Arrows point to the future oocyte. Scale bars, 10µm.

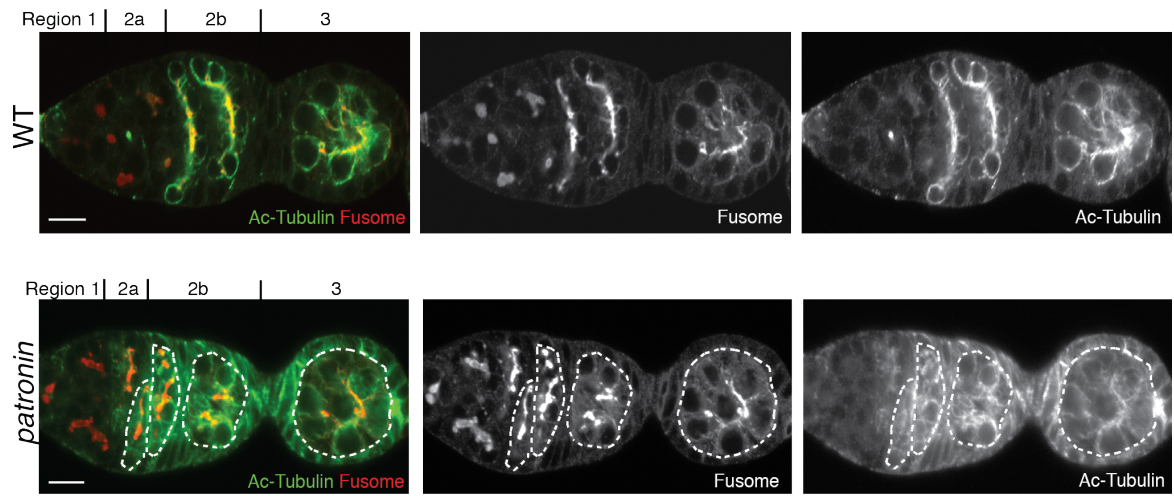


Fig. S3. Patronin stabilises microtubules in the cyst. Wild type (WT; top) and *patronin* mutant (bottom) cysts stained with anti-acetylated tubulin (Ac-Tubulin) and anti-Shot (Fusome). Mutant cysts are marked by dashed lines. Regions of the germarium are indicated on the top. Scale bars, 10 μ m.

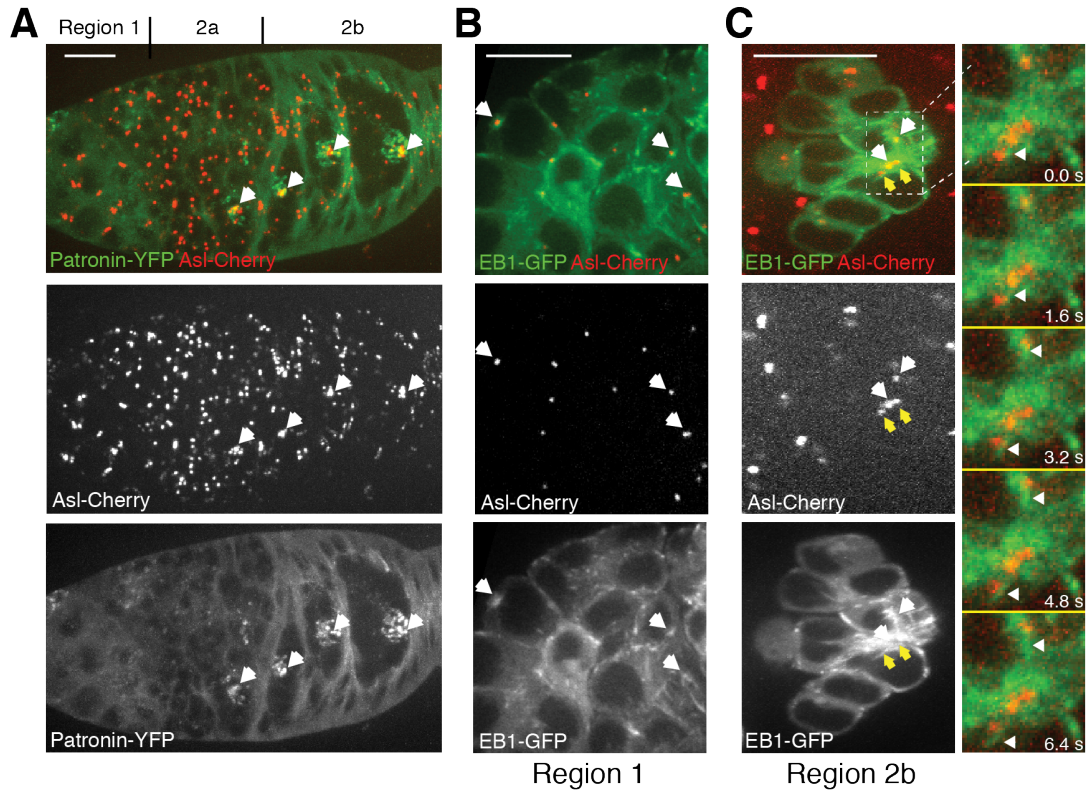
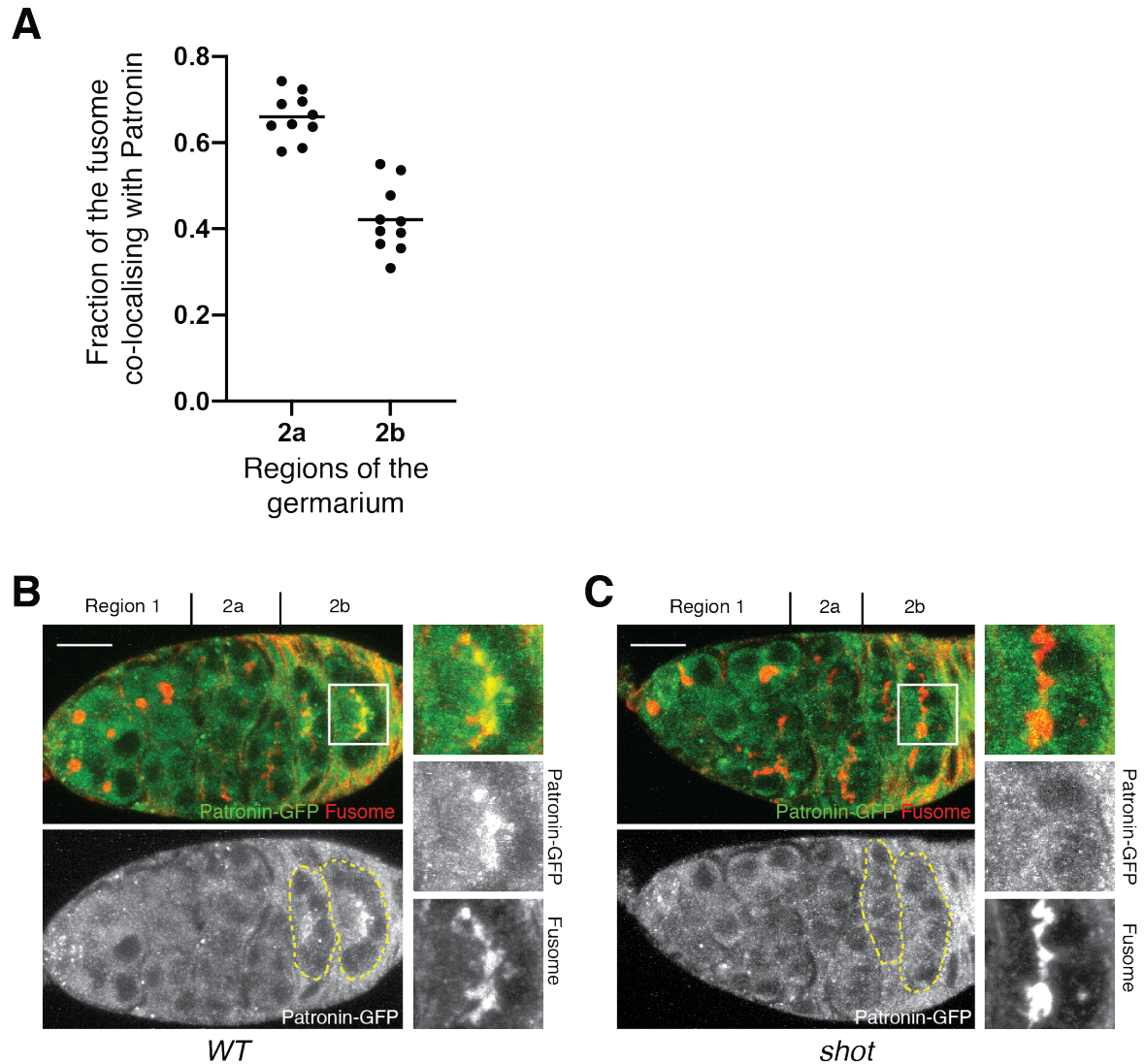


Fig. S4. Patronin MTOCs are not centrosomal. (A) Patronin foci lie outside the centrosomal cluster. Live gerarium expressing Patronin-YFP and a centrosomal protein Asterless-Cherry (Asl-Cherry). The image is a projection of several z sections spanning the cyst. Arrows mark centrosomal clusters. (B-D) Centrosomes contribute to microtubule organisation in the cyst. Live geraria expressing EB1-GFP and Asterless-Cherry (Asl-Cherry). (B) Region 1 of the gerarium. The image is taken from Movie S5. Arrows indicate active centrosomes. (C) Region 2b of the gerarium. The images are projections of several time points from Movie S6. White arrows point to two active centrosomes in the presumptive oocyte. Yellow arrows point to two inactive centrosomes. Close-ups are still images from Movie S6. Arrowheads show new EB1-GFP comets emanating from the active centrosomes. Scale bars, 10μm.



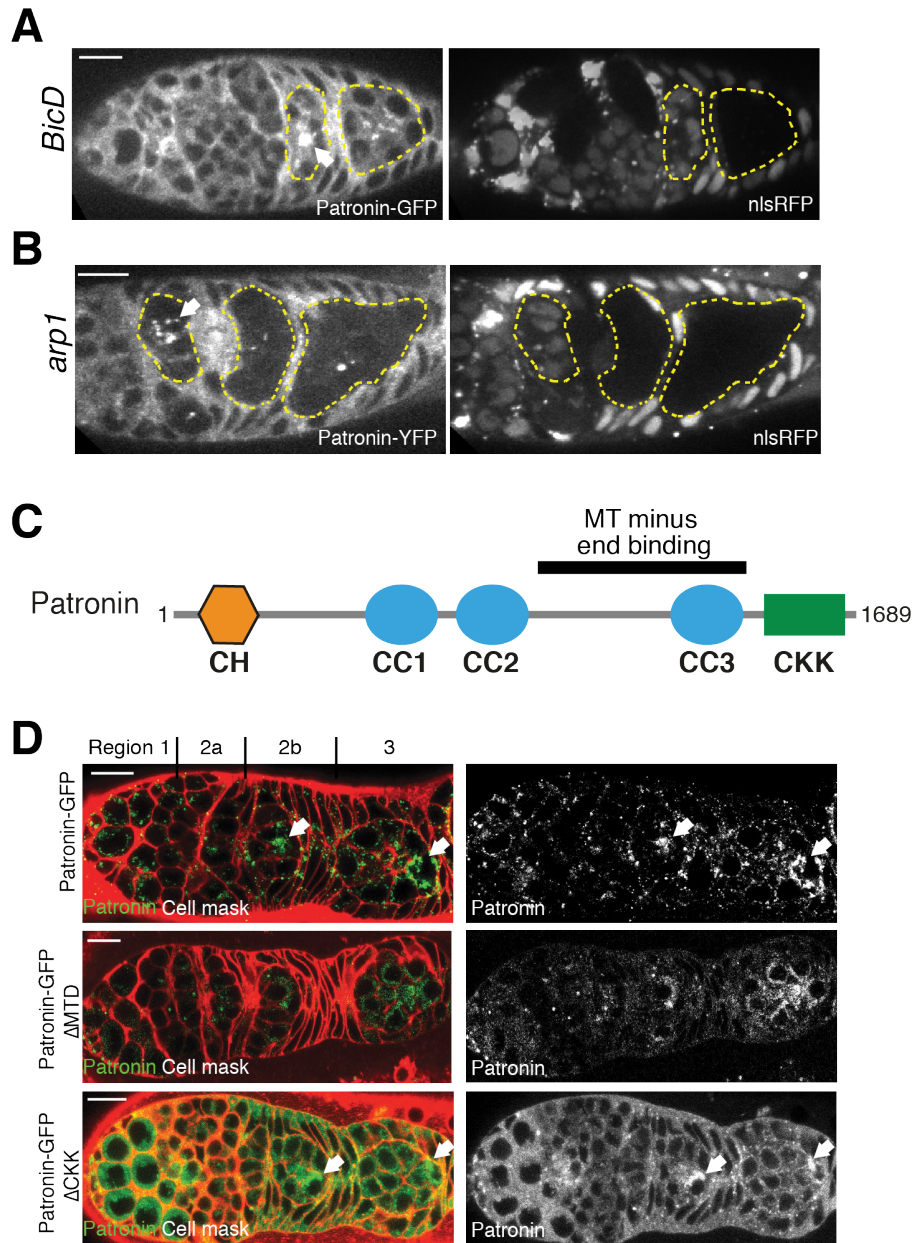


Fig. S6. Patronin localisation depends on Dynein activity and MT minus end binding. (A-B) Live germaria containing *BicD* (A) or *arp1* (B) mutant cysts expressing transgenic Patronin-GFP (A) or Patronin-YFP (B). Cyst are indicated by dashed lines. Mutant cysts are marked by the absence of nlsRFP. Arrows indicate wild type cysts. (C) A diagram showing the domain structure of Patronin. (D) The MT minus end binding domain (MTD) is required for Patronin localisation. Live germaria expressing wild type (top), MTD-deleted (middle) or CKK-deleted (bottom) transgenic Patronin-GFP. Cell membranes are labelled by CellMask. Arrows indicate accumulation of Patronin foci in the presumptive oocyte. Regions of the germarium are indicated on the top. Scale bars, 10 μ m.

Movie S1. A time-lapse video of the microtubule plus-end binding protein EB1-GFP in wild-type germline cysts in region 2 of the germaium. The red line outlines the cells containing MTOCs. Related to Figure 3B. Images were collected every 1 second on a spinning disc confocal microscope. The video is shown at 15 frames/sec.

Movie S2. A time-lapse video of the microtubule plus-end binding protein EB1-GFP in wild-type germline cysts in region 3. Related to Figure 3B. Images were collected every 1 second on a spinning disc confocal microscope. The video is shown at 15 frames/sec.

Movie S3. A time-lapse video of the microtubule plus-end binding protein EB1-GFP in *patronin* mutant germline cysts in region 2. Related to Figure 3B. Images were collected every 1 second on a spinning disc confocal microscope. The video is shown at 15 frames/sec.

Movie S4. A time-lapse video of the microtubule plus-end binding protein EB1-GFP in *patronin* mutant germline cysts in region 3. Related to Figure 3B. Images were collected every 1 second on a spinning disc confocal microscope. The video is shown at 15 frames/sec.

Movie S5. A time-lapse video of the microtubule plus-end binding protein EB1-GFP (green) and the centrosomal protein Asterless-Cherry (red) in wild-type germline cysts in region 1. Arrowheads point to active centrosomes. Related to Figure S4B. Images were collected every 1.6 seconds on a spinning disc confocal microscope. The video is shown at 15 frames/sec.

Movie S6. A time-lapse video of the microtubule plus-end binding protein EB1-GFP (green) and centrosomal protein Asterless-Cherry (red) in wild-type germline cysts in region 2b. The white arrow points to an active centrosome in the presumptive oocyte. Related to Figure S4C. Images were collected every 1.6 seconds on a spinning disc confocal microscope. The video is shown at 15 frames/sec.

References and Notes

1. K. Lu, L. Jensen, L. Lei, Y. M. Yamashita, Stay Connected: A Germ Cell Strategy. *Trends Genet.* **33**, 971–978 (2017).
2. L. Lei, A. C. Spradling, Mouse primordial germ cells produce cysts that partially fragment prior to meiosis. *Development.* **140**, 2075–2081 (2013).
3. L. Lei, A. C. Spradling, Mouse oocytes differentiate through organelle enrichment from sister cyst germ cells. *Science.* **352**, 95–99 (2016).
4. M. de Cuevas, M. A. Lilly, A. C. Spradling, Germline cyst formation in *Drosophila*. *Annu. Rev. Genet.* **31**, 405–28 (1997).
5. J. Huynh, D. StJohnston, The Origin of Asymmetry: Early Polarisation of the *Drosophila* Germline Cyst and Oocyte. *Current Biology.* **14**, R438–R449 (2004).
6. W. E. Theurkauf, B. M. Alberts, Y.-N. Jan, T. A. Jongens, A central role for microtubules in the differentiation of *Drosophila* oocytes. *Development.* **118**, 1169–1180 (1993).
7. M. McGrail, T. S. Hays, The microtubule motor cytoplasmic dynein is required for spindle orientation during germline cell divisions and oocyte differentiation in *Drosophila*. *Development.* **124**, 2409–2419 (1997).
8. J. Bolívar *et al.*, Centrosome migration into the *Drosophila* oocyte is independent of BicD and egl, and of the organisation of the microtubule cytoskeleton. *Development.* **128**, 1889–1897 (2001).
9. W. Meng, Y. Mushika, T. Ichii, M. Takeichi, Anchorage of microtubule minus ends to adherens junctions regulates epithelial cell-cell contacts. *Cell.* **135**, 948–959 (2008).
10. A. J. Baines *et al.*, The CKK Domain (DUF1781) Binds Microtubules and Defines the CAMSAP/sps4 Family of Animal Proteins. *Molecular Biology and Evolution.* **26**, 2005–2014 (2009).
11. S. S. Goodwin, R. D. Vale, Patronin Regulates the Microtubule Network by Protecting Microtubule Minus Ends. *Cell.* **143**, 263–274 (2010).
12. N. Tanaka, W. Meng, S. Nagae, M. Takeichi, Nezha/CAMSAP3 and CAMSAP2 cooperate in epithelial-specific organization of noncentrosomal microtubules. *Proc Natl Acad Sci USA.* **109**, 20029–20034 (2012).
13. D. Nashchekin, A. R. Fernandes, D. St Johnston, Patronin/Shot Cortical Foci Assemble the Noncentrosomal Microtubule Array that Specifies the *Drosophila* Anterior-Posterior Axis. *Dev Cell.* **38**, 61–72 (2016).
14. V. Lantz, J. S. Chang, J. I. Horabin, D. Bopp, P. Schedl, The *Drosophila orb* RNA-

- binding protein is required for the formation of the egg chamber and establishment of polarity. *Genes Dev.* **8**, 598–613 (1994).
15. A. P. Mahowald, J. M. Strassheim, Intercellular migration of centrioles in the germarium of *Drosophila melanogaster*. An electron microscopic study. *The Journal of Cell Biology.* **45**, 306–320 (1970).
 16. N. C. Grieder, M. de Cuevas, A. C. Spradling, The fusome organizes the microtubule network during oocyte differentiation in *Drosophila*. *Development.* **127**, 4253–4264 (2000).
 17. K. Roper, N. H. Brown, A spectraplakins is enriched on the fusome and organizes microtubules during oocyte specification in *Drosophila*. *Curr Biol.* **14**, 99–110 (2004).
 18. H. Lin, L. Yue, A. C. Spradling, The *Drosophila* fusome, a germline-specific organelle, contains membrane skeletal proteins and functions in cyst formation. *Development.* **120**, 947–956 (1994).
 19. M. De Cuevas, A. C. Spradling, Morphogenesis of the *Drosophila* fusome and its implications for oocyte specification. *Development.* **125**, 2781–2789 (1998).
 20. K. Jiang *et al.*, Microtubule minus-end stabilization by polymerization-driven CAMSAP deposition. *Dev Cell.* **28**, 295–309 (2014).
 21. H. Lin, A. C. Spradling, Fusome asymmetry and oocyte determination in *Drosophila*. *Developmental Genetics.* **16**, 6–12 (1995).
 22. C. Navarro, H. Puthalakath, J. M. Adams, A. Strasser, R. Lehmann, Egalitarian binds dynein light chain to establish oocyte polarity and maintain oocyte fate. *Nat Cell Biol.* **6**, 427–435 (2004).
 23. B. Suter, R. Steward, Requirement for phosphorylation and localization of the Bicaudal-D protein in *Drosophila* oocyte differentiation. *Cell.* **67**, 917–926 (1991).
 24. R. Nieuwburg *et al.*, Localised dynactin protects growing microtubules to deliver oskar mRNA to the posterior cortex of the *Drosophila* oocyte. *Elife.* **6**, e27237 (2017).
 25. M. C. Hendershott, R. D. Vale, Regulation of microtubule minus-end dynamics by CAMSAPs and Patronin. *Proceedings of the National Academy of Sciences.* **111**, 5860–5865 (2014).
 26. M. E. Pepling, A. C. Spradling, Female mouse germ cells form synchronously dividing cysts. *Development.* **125**, 3323–3328 (1998).
 27. K. Roper, N. H. Brown, Maintaining epithelial integrity: a function for gigantic spectraplakins isoforms in adherens junctions. *Journal of Cell Biology.* **162**, 1305–1315 (2003).

28. B. Ran, R. Bopp, B. Suter, Null alleles reveal novel requirements for Bic-D during *Drosophila* oogenesis and zygotic development. *Development*. **120**, 1233–1242 (1994).
29. S. T. Thibault *et al.*, A complementary transposon tool kit for *Drosophila melanogaster* using P and piggyBac. *Nature Genetics*. **36**, 283–287 (2004).
30. T. Schupbach, E. Wieschaus, Female sterile mutations on the second chromosome of *Drosophila melanogaster*. II. Mutations blocking oogenesis or altering egg morphology. *Genetics*. **129**, 1119–1136 (1991).
31. F. Port, H.-M. Chen, T. Lee, S. L. Bullock, Optimized CRISPR/Cas tools for efficient germline and somatic genome engineering in *Drosophila*. *Proceedings of the National Academy of Sciences*. **111**, E2967–76 (2014).
32. N. Lowe *et al.*, Analysis of the expression patterns, subcellular localisations and interaction partners of *Drosophila* proteins using a pigP protein trap library. *Development*. **141**, 3994–4005 (2014).
33. G. B. Gloor, N. A. Nassif, D. M. Johnson-Schlitz, C. R. Preston, W. R. Engels, Targeted gene replacement in *Drosophila* via P element-induced gap repair. *Science*. **253**, 1110–1117 (1991).
34. P. T. Conduit, A. Wainman, Z. A. Novak, T. T. Weil, J. W. Raff, Re-examining the role of *Drosophila* Sas-4 in centrosome assembly using two-colour-3D-SIM FRAP. *Elife*. **4** (2015), doi:10.7554/eLife.08483.
35. T. Zhao, O. S. Graham, A. Raposo, D. St Johnston, Growing microtubules push the oocyte nucleus to polarize the *Drosophila* dorsal-ventral axis. *Science*. **336**, 999–1003 (2012).
36. H. Wang, I. Brust-Mascher, G. Civelekoglu-Scholey, J. M. Scholey, Patronin mediates a switch from kinesin-13-dependent poleward flux to anaphase B spindle elongation. *The Journal of Cell Biology*. **4**, 1343 (2013).
37. T. B. Chou, N. Perrimon, Use of a yeast site-specific recombinase to produce female germline chimeras in *Drosophila*. *Genetics*. **131**, 643–653 (1992).